

# Laser Controllable Growth of Graphene via Ni-Cu Alloy Composition Modulation

Xiaohui Ye<sup>1</sup> · Zhe Lin<sup>1</sup> · Hongjun Zhang<sup>1</sup> ·  
Hongwei Zhu<sup>1</sup> · Minlin Zhong<sup>1</sup>

Accepted: 21 August 2015 / Published online: 10 September 2015  
© Springer New York 2015

**Abstract** Graphene has many unique properties, most of them strongly depend on the number of layers. It is significant to develop a facile approach to realize the controllable growth of graphene with specific number of layers. We ever reported an efficient approach to grow graphene rapidly and locally by laser irradiation. In this work, we offers yet another important feature, to control the number of layers of graphene. Ni-Cu alloy has been reported to be used successfully as the catalyst for graphene growth with controllable number of layers. In that case, the Ni-Cu alloys with different compositions were normally formed by thermal evaporation. Here we provide an efficient way to fabricate the Ni-Cu alloy catalysts by laser cladding. Then the high power laser was employed to melt the Ni and Cu mixed powders. Different Ni-Cu alloy catalysts were formed in a high rate of 720 mm<sup>2</sup>/min with a thickness of 1.2 mm. Then the graphene with controllable layers was rapidly and locally grown on the Ni-Cu catalysts by laser irradiation at a high rate (18 cm<sup>2</sup>/min) at room temperature. We found that the Ni-Cu catalyst with 15 % Cu could be helpful to grow single layer graphene, which occupied 92.4 % of the entire film. Higher Cu content didn't promote the growth due to the oxygen involved during the growth process. The controllable growth mechanism of graphene by laser processing was discussed. Combining the rapid catalyst fabrication and graphene synthesis make it a cost- and time-efficient method to produce the controllable graphene films.

**Keywords** Graphene · Laser rapid synthesis · Controllable layer · Ni-Cu alloy · Laser cladding

---

✉ Minlin Zhong  
zhml@tsinghua.edu.cn

<sup>1</sup> School of Materials Science and Engineering, Tsinghua University, Beijing 100084, China

## Introduction

Graphene a single layer or few layers of carbon atoms tightly packed into a two-dimensional (2D) honeycomb lattice, is a basic building block of all graphitic forms [1,2]. Currently, graphene is a rapidly rising star, owing to its exceptional properties, e.g., ultra-high electrical conductivity, excellent thermal stability, and extraordinary mechanical properties. The outstanding properties of graphene make it a unique material for many potential applications [3–5], including next generation ultra-compact computers, flat screen displays, sensors, solar cells, conducting plastics or ceramics, micro-electro-mechanical devices and novel protection coatings [6–9].

The distinct properties of graphene strongly depend on its layers. Raman spectra for single layer, bilayer, and multilayer are different [10–12], reflecting the changes in their electron bands. The optical transparency of monolayer graphene can reach up to 97.7 %. The opacity increases with membranes' thickness, and each graphene layer adds 2.3 % [13]. The electrical properties and structures of single layer, bilayer, and multilayer graphene show huge differences. The electrical resistance decrease as the number of layers increases [14]. Owing to the specific properties, the graphene with different layers can be applied to various fields. The single-layer graphene has a zero band gap, and its conduction and valence bands are shaped like an inverted pair of cones that meet in a single point at  $E=0$  in momentum space [15]. Due to the special structure, the carrier mobility of single-layer graphene is extremely high ( $2 \times 10^5$  cm<sup>2</sup>/vs) [5,7]. The actual single-layer graphene is synthesized through exfoliation of highly oriented pyrolytic graphite (HOPG), which is for fundamental research due to the small size of graphene obtained. As for bilayer graphene, it has a continuously tunable band gap under electric field and shows unique quantum-mechanical behavior. It makes that bilayer graphene has great potential application for optoelectronics and microprocessors [15–18]. Once the number of layers exceeds ten, graphene film would share a band structure similar to graphite [15,19]. To realize the specific properties, it is significant to develop a controllable approach to grow the graphene with specific number of layers for practical applications.

One of the most important parameters of graphene growth is specific catalyst. For now, the following metals have been used as growth catalysts, i.e., Ru, Ir, Co, Re, Ni, Cu, Pt, Pd [20–24]. Among them, Ni and Cu are the most widely-used metals. For Ni, the carbon sources are dissolved into the metal at high temperature. With the temperature cooling down, the solubility of C in Ni decreases and the extra carbon sources then precipitate out on the Ni surface to form graphene. During this processing, the precipitation of carbon sources cannot be controlled, so that the thickness of graphene is uncontrollable [24]. While, due to the indissolubility of C in Cu, it is very easy to grow single-layer graphene on Cu. The carbon sources are mainly absorbed by Cu atoms at high temperature, and then the single-layer graphene is formed on the surface [24]. Combining these two growth mechanisms, we can realize the controllable growth of graphene. Several approaches for synthesizing controllable graphene have been developed. Liu, et al. [20] reported a new technique to synthesis

graphene, called universal segregation growth. They obtained graphene wafers from Ni, Co, Fe, Cu and Cu-Ni alloy films via thermal annealing by introducing carbon sources. They demonstrated that monolayer and bilayer graphene films were grown on Cu-Ni alloy by combining the distinct segregation behaviors of Cu and Ni. Then they studied the relationship of graphene layer and the content of Ni and Cu in the alloy [15]. They found that increasing the atomic percentage of Cu in Ni-Cu alloy tended to segregate thinner uniform graphene. Dai, et al. [21] used a Ni-Mo alloy to suppress the carbon precipitation and activates a self-limited growth for homogeneous monolayer graphene. A similar work by Weatherup et al. [22] reported that Au-Ni alloy was prepared for the large single crystal growth. Besides altering the composition of the catalysts, Chen et al. [14] controlled the graphene thickness by varying the deposition temperature and cooling rate, but also on Ni-Cu alloy foils. A high cooling rate and less deposition time would be helpful to grow single layer graphene. Laser cladding is a hard facing process that uses a high-powered laser beam to melt the coating material and a thin layer of the substrate to form a pore- and crack-free coating [25–27]. It is a convenient way to fabricate the alloy coating. Varying the proportion of original materials, the different alloy coatings would be obtained.

With these approaches, it is feasible to control the thickness of graphene by modulating the composition of the binary alloy as the catalytic catalyst. However, almost all of the catalyst was fabricated by thermal evaporation, which is a time-consuming approach with the limited thickness of catalyst. Meanwhile, the synthesis of graphene was always involved a high temperature process for a long time to segregate carbon atoms. We ever reported an efficient approach to grow graphene rapidly and locally by laser irradiation [23]. This laser approach combines lots of merits, i.e., large-area growth, patterned graphene and fast growth for practical applications. In that reported work, graphene was synthesized by laser irradiation on solid carbon source coated on nickel surface in ambient condition. The rapid solidification made it possible to grow graphene at a high rate compared to conventional approaches. Arbitrary patterns designed by computer aided design (CAD) software were fabricated directly on Ni substrates without additional mask or setup. Together the rapid heating and cooling made a cost- and time-efficient and eco-friendly method to produce high-quality graphene films [23].

Integrated with above work, we further introduce here the graphene layer control by modulating the composition of the catalyst substrate. We used a high power density continuous wave (CW) fiber laser to deposit a composition-designable Ni-Cu alloy onto a substrate. The Ni-Cu alloy was deposited in a high rate up to  $720 \text{ mm}^2/\text{min}$  with a changeable thickness up to 1.2 mm. Then the laser was further applied to growth the graphene as reported earlier. The high power laser radiated the Ni-Cu surface together with the as-coated carbon with a very high heating rate up to a temperature of  $\sim 1600 \text{ }^\circ\text{C}$ , formed a large-area bath and then cooled down at a very high cooling rate. The rapid solidification made it possible to grow graphene at a high rate ( $18 \text{ cm}^2/\text{min}$ ). In addition to the merits of graphene growth by laser, e.g., large-area growth, patterned growth and mass production, in this work, we offers yet another important feature, to control the number of layers of graphene.

## Material and Methods

### Ni-Cu Alloy with Specific Composition

In this study, we first focus on the influence of catalyzers on graphene growth. Based on the mechanism of precipitation growth, it is feasible to control graphene layers by varying the proportion of Cu and Ni in catalyst [15,20–22]. Figure 1a shows the schematic of Ni-Cu catalyst fabrication by laser cladding. High power density continuous wave fiber laser was employed to fabricate the catalyst. High pure (99.99 %) Cu and Ni powders of uniform size, about 75  $\mu\text{m}$  in varying proportions (listed in Table 1) were assembled into a side shaft powder feeding apparatus (BAMTRI, DPSF-2). With the assistance of airflow, the pre-mixed powders were delivered into the irradiated area by laser beam. The substrate can be any commonly used metals. Almost at the same time, the mixed powders and the substrate were heated and melted caused by laser irradiation. The molten powders then dropped down into the bath just forming in the substrate surface. Once the laser moved forward, the Ni-Cu alloy coating was formed on the substrate surface. The quality of Ni-Cu catalyst strongly depended on laser power density, scanning rate and powder feeding rate. Table 1 lists the optimal conditions for different catalysts, and the number in the first column represents the content of Cu.

### Controllable Graphene Synthesis by Laser Irradiation

The catalysts were prepared and then polished to a smooth and flat surface. The graphite powders with uniform size of  $\Phi 50$  nm were used as the carbon source. These nano-powders were mixed with alcohol (analytical reagent) to form a suspension. The mixed ratio was 1.0 g powders with 1.6 ml alcohol. Then, the spin coater (SC-1B) was applied to prepare the carbon coatings with the thickness of  $\sim 20$   $\mu\text{m}$ . The fiber laser were employed to scan the pre-coated carbon source on the Ni-Cu catalysts, as shown in Fig. 1b. In this approach, the Ni-Cu surface together with the as-coated carbon is heated at a high rate up to  $\sim 2000$   $^{\circ}\text{C}$ , forming a bath and then cools down at rate up to

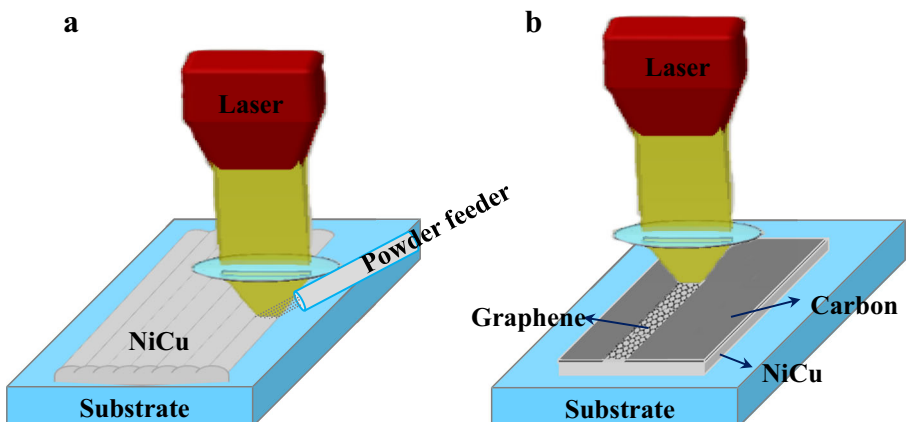


**Fig. 1** Schematic of **a** Ni-Cu catalyst fabrication by laser cladding. **b** Layer controllable graphene synthesis

**Table 1** The optimal conditions for different catalysts

Sample	Composition (wt. %)		Power density (W/cm <sup>2</sup> )	Scanning rate (mm/s)	Powder feeding rate (g/min)
	Cu	Ni			
Cu0	0	100	$2.15 \times 10^4$	4	13.33
Cu5	5	95	$2.15 \times 10^4$	4	13.33
Cu15	15	85	$2.15 \times 10^4$	4	13.33
Cu25	25	75	$2.12 \times 10^4$	4	13.33
Cu35	35	65	$2.00 \times 10^4$	4	13.33
Cu50	50	50	$1.85 \times 10^4$	4	13.33
Cu75	75	25	$1.58 \times 10^4$	4	13.33

$10^3 \sim 10^4$  °C/s. When the laser was shut off, graphene could be available immediately. The formation of graphene was implemented by fiber laser with a Gauss beam of  $\Phi 3$  mm. The laser power density was  $14.1 \times 10^3$  W/cm<sup>2</sup>, and the scanning rate was 60 cm/min with 25 L/min argon (99.99 %) as shielding gas.

## Characterization

The component distributions of the Ni-Cu catalysts were detected by energy dispersive X-ray spectroscopy (EDS). The structures of catalysts were characterized by X-ray diffraction (XRD, Bruker, D8 Advance), from 20 to 100° with scanning rate of 8°/min. As-grown graphene were characterized by optical microscopy, scanning electron microscopy (SEM, LEO-1530), Raman spectroscopy (Renishaw 2000), Raman imaging spectroscopy (Nanophoton, Raman-11), and auger electron spectroscopy (AES, ULVAC-PHI, PHI-700). The topography of graphene was observed by optical and SEM images. The layer number of graphene was identified by Raman spectra and AES.

## Results and Discussion

### Composition of Ni-Cu Alloy Modulated by Laser Cladding

Ni-Cu catalysts were prepared by laser cladding successfully. Figure 2a shows the macrograph of Ni-Cu alloy after laser cladding. The good formation of Ni-Cu alloy without pores or cracks was obtained under the optimal condition. The component distributions were analyzed by EDS, as shown in Figs. 2b and g and Table 2. The red images present Cu distributions and the green ones are Ni distributions. The color images show that there are uniform distributions of Cu and Ni in each sample. The actual compositions are listed in Table 2. It can be observed the loss of Cu and introduction of oxygen, due to high temperature and open condition during laser cladding. However, the small loss of Cu could be acceptable. The EDS results show that the catalysts prepared by laser cladding are homogenous.

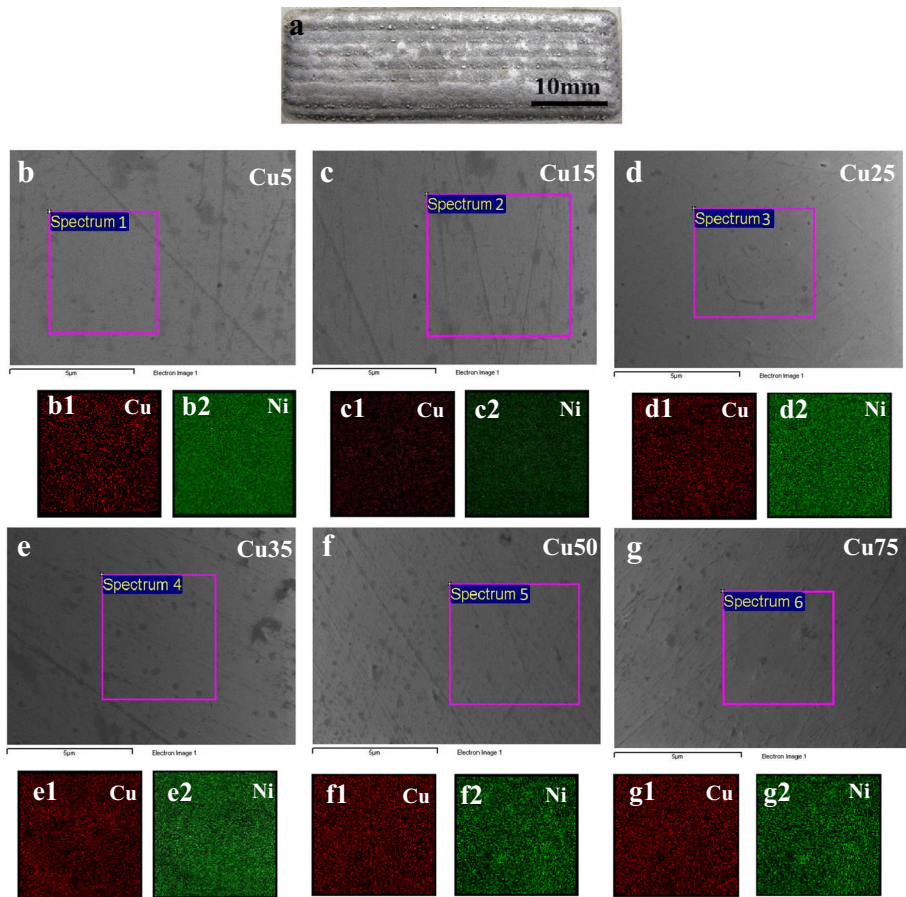


**Fig. 2** a Macrograph of Ni-Cu alloy. b-g Cu and Ni distributions of different catalysts. The red images present Cu distributions and the green ones show Ni distributions

XRD was used for catalyst structure analysis. Figure 3a shows the spectra of different catalysts with Cu increasing from bottom to up. Four characteristic peaks can be observed, calibrated as (111), (200), (220) and (311) of face-centered cubic (*fcc*).

**Table 2** The actual composition in each catalyst

Sample	Actual composition		
	Cu (wt. %)	Ni (wt. %)	O (wt. %)
Cu5	3.3	96.7	0
Cu15	13.01	86.42	0.57
Cu25	22.83	76.4	0.77
Cu35	31.94	67.26	0.8
Cu50	39.1	59.85	1.05
Cu75	73.91	22.73	3.36

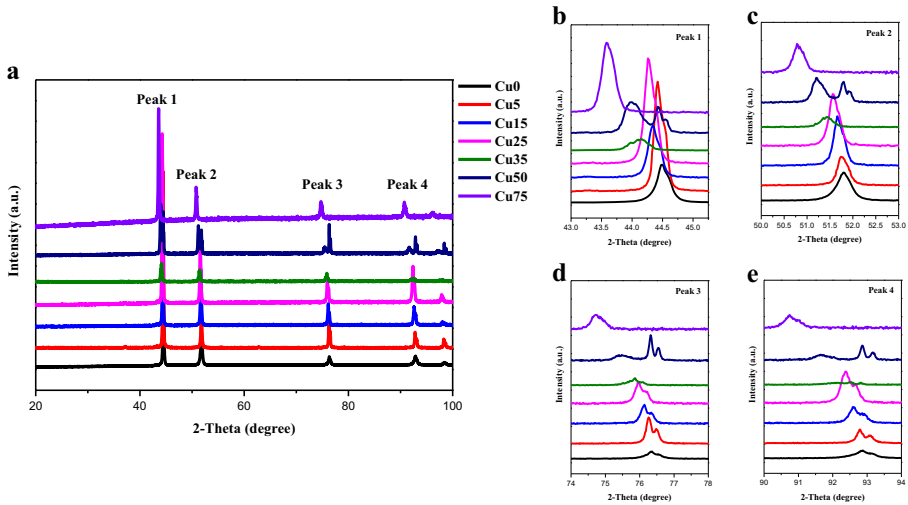


**Fig. 3** a XRD spectra of different catalysts. b, c, d and e represent different peaks in a, respectively

The similar spectra demonstrate that the structures of all the samples are the same, i.e., *fcc*, meaning that the structure of Ni-Cu alloy is close to that of pure Ni (the bottom spectrum). However, it is also different from each other. Figures 3b and e display the four characteristic peaks respectively, and all these peaks shift left as Cu increasing. The left shift implies the increasing of interplanar spacing. For *fcc*, the larger interplanar spacing equals to a bigger structure cell. The reason for the left shift is that pure Cu has a bigger structure cell (lattice constant  $a_{\text{Cu}}=3.6149 \text{ \AA}$ ) than pure Ni (lattice constant  $a_{\text{Ni}}=3.5238 \text{ \AA}$ ). Consequently, the structure is closer to that of pure Cu as the Cu content increases.

### Controllable Graphene Growth by Laser Irradiation

The graphene fabrication was implemented by fiber laser direct irradiation on the prepared Ni-Cu alloy catalysts. With the radiation, the Ni-Cu surface together with the as-coated carbon is heated at a rate of up to  $10^4 \text{ }^\circ\text{C/s}$  to a temperature of around  $2000 \text{ }^\circ\text{C}$ , forming a large-area bath and then cools down at rate of up to  $10^3 \sim 10^4 \text{ }^\circ\text{C/s}$ . The topography of graphene was characterized by optical microscopy and SEM, as seen in Fig. 4. There are amount of tiny strips on the pure Ni surface (Cu0) (Fig. 4a). The magnified SEM image shows the obvious wrinkles of graphene (Fig. 4h). Once Cu added, the strips are much less than that of pure Ni, as seen in Fig. 4b, c, i and j. When the content of Cu came to 25 % and 35 %, graphene films turned to discontinuous, as shown in Fig. 4d, e, k and l. For Cu50 and Cu75, the wrinkles of graphene cannot be observed any more (Fig. 4f, g, m and n). It is hard to tell whether it is graphene or not by these topographies, due to the loss of graphene typical topography. The information of topography demonstrate that appropriate ratio of Cu/Ni, i.e., Cu of 5 % and 15 %, can be helpful for formation continuous graphene films, rather than higher content of Cu (25 % and over).

Raman spectroscopy is an efficient way to characterize carbon materials. Ferrari et al. [10] pointed out that G band ( $\sim 1580 \text{ cm}^{-1}$ ) reflects the doubly degenerate zone



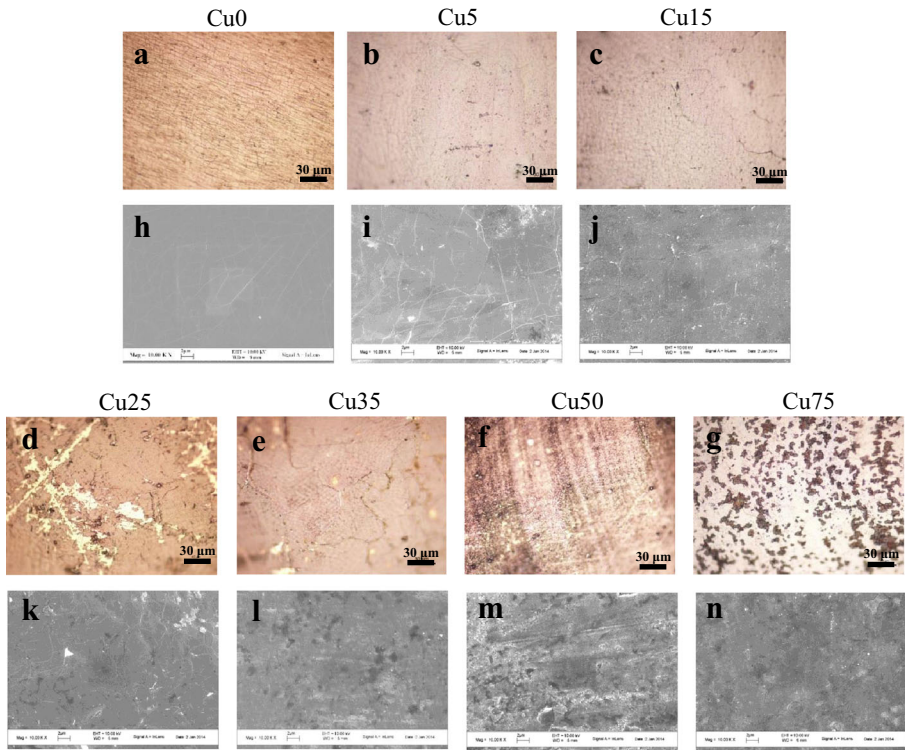


**Fig. 4** Topography of graphene on different catalysts. **a-g** optical images. Share the same scale bar of 30  $\mu\text{m}$ . **h-n** SEM images. Scale bars: 5  $\mu\text{m}$

center  $E_{2g}$  mode while D band ( $\sim 1350\text{ cm}^{-1}$ ) indicates the absence of a significant number of defects. The 2D band ( $\sim 2700\text{ cm}^{-1}$ ) provides information about the number of layers. The increase in layers leads to a significant decrease of the relative intensity of 2D ( $I_{2D}$ ) with a blue shift. Here, we performed Raman imaging and Raman spectra to figure out the relationship between catalysts and graphene layers. Figures 5a and g display the  $I_{2D}/I_G$  mapping results in an area of  $254 \times 25\ \mu\text{m}^2$ . The lighter color represents a higher value of  $I_{2D}/I_G$  and the dark blue represents a lower one. Raman spectra were extracted from the Raman imaging accordingly, as shown in Figs. 5h and n. The ratio of  $I_{2D}/I_G$  greater than 1.0 was calculated from the Raman mapping software, which means that 2D peak intensity is greater than G peak. This is the typical trait of monolayer or bilayer (1–2 L) graphene. So the ratio of  $I_{2D}/I_G$  greater than 1.0 equals to the ratio of 1–2 layer graphene (Fig. 5o). Based on the relationship between the relative intensity of 2D ( $I_{2D}$ ) and graphene layers, a higher  $I_{2D}/I_G$  implies a lower number of graphene layers. For the pure Ni catalyst (Cu0), most of the detection area was covered by multilayer graphene films, and the occupancy of 1–2 L graphene is 58.8 %. With 5 % Cu adding into the catalyst, 1–2 L graphene occupied up to 78.7 % of all the detection area. 15 % Cu of Ni-Cu alloy brought a high Ratio of 1–2 L graphene, up to 92.4 %. Meanwhile, the higher Cu content, e.g., 25 % and 35 %, could not keep a higher occupancy of 1–2 L graphene, and the 1–2 L graphene ratios are 70.2 % and 64.3 %. When Cu content is over 50 %, there is no typical trait of graphene from the



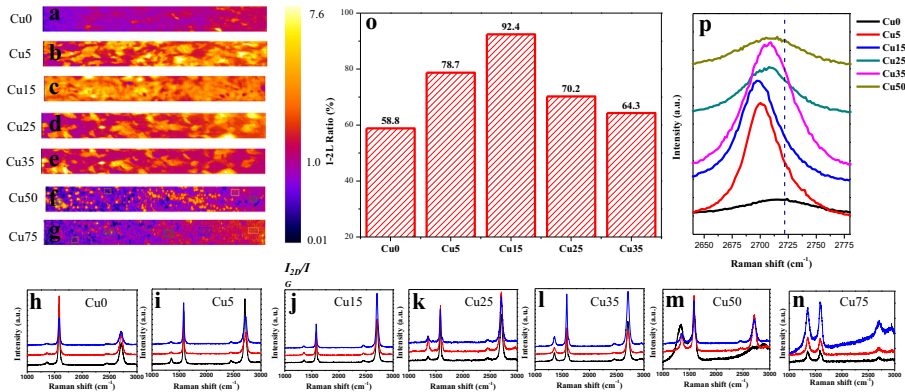


**Fig. 5** a–g 532 nm Raman imaging of  $I_{2P}/I_G$ . h–n Raman spectra extracted from the Raman imaging accordingly. o The ratio of 1–2 layer graphene occupied in different samples. (p) 2D peak position shift of different samples

Raman spectra. Figure 5p shows the position shift of 2D peak. Compared to Cu0, there was  $24\text{ cm}^{-1}$  red shift of Cu5 and  $29\text{ cm}^{-1}$  red shift of Cu15. Cu25 and Cu35 had slight red shift,  $8\text{ cm}^{-1}$  and  $9\text{ cm}^{-1}$ , respectively. The red shift of 2D peak demonstrated the decrease of graphene layers.

AES depth profile analysis was employed to study the element distributions from surface to a depth of 6 nm, by using a sputtering rate 2 nm/min. The depth profile of element C can be used to identify the number of graphene layer. Every layer of graphene is 0.34 nm. Figure 6 provides the depth profiles of C, O, Ni and Cu in different catalysts. Here, we considered the depth where C dropped down and Ni rose up as the thickness of graphene. It can be seen (Fig. 6a) that for pure Ni, C remains a high proportion ( $>60\%$ ) in the whole depth of 6 nm, and there is no cross point with the Ni distribution line, meaning that the thickness of graphene is more than 6 nm. In this case, the graphene would be multilayer films. Figures 6b, c and d show the significant drop of C and obvious rise of Ni at 0.75, 0.5, and 0.98 nm, respectively. Accordingly, the layers of graphene would be 2 L, 1 L and 3 L. These results demonstrate that the catalyst with 15 % Cu is the most appropriate substrate to grow single-layer graphene; the bilayer graphene tend to be grown on the catalyst with 5 % Cu; the catalyst with 25 % Cu is available for tri-layer graphene. Figure 6e also shows a higher of C content than Ni and Cu in the whole profile. The controllable growth by Cu addition doesn't work anymore, when Cu is over 35 %.

### Mechanism of Controllable Graphene Growth by Laser Irradiation

From the above results, the Ni-Cu catalysts can effectively control the growth of graphene. The appropriate Cu content (5 % and 15 %) is helpful to form continuous and large-area 1–2 L graphene films. Once the content of Cu reached 25 % and 35 %, the graphene turned to heterogeneous and multilayer. A higher Cu content, like 50 % and 75 %, could not grow graphene successfully. These results are so different from the other reports. Usually, the higher Cu content leads to the higher coverage of 1–2 L graphene [15,20], and the pure Cu can easily grow the single layer graphene. However, in this work, the higher Cu is invalid to control the graphene growth. As studied before

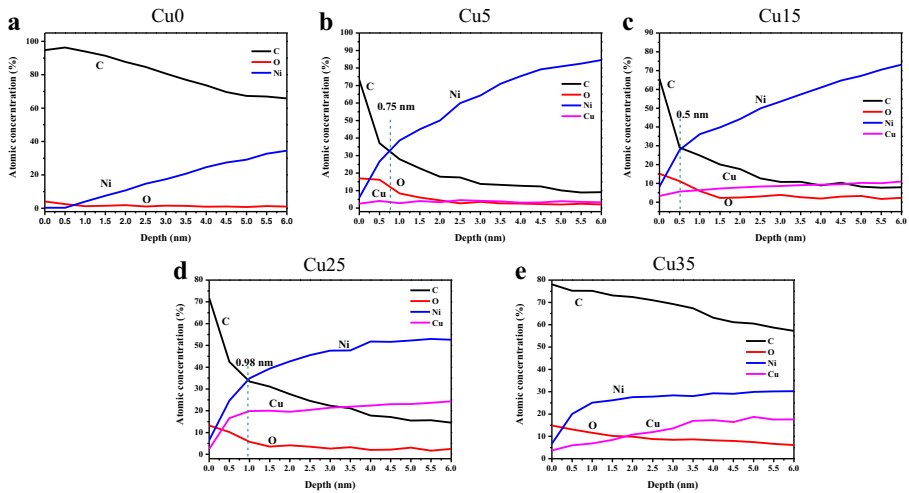


**Fig. 6** Depth profiles of C, O, Ni and Cu by AES analysis. **a** Cu0; **b** Cu5; **c** Cu15; **d** Cu25; **e** Cu35

[24,28–31], there are two different growth mechanism of graphene on Ni and Cu. Graphene is grown on Cu by surface absorbed. It is an easy way to grow the single-layer graphene. Multilayer graphene is grown on Ni by carbon atoms precipitation from the bulk out to the surface. Figure 7 shows the schematic of mechanism of controllable growth. Here, both of the two kinds of growth mode were involved to realize a controllable growth. In lower Cu case, the controllable growth was similar with other works [15, 20]. In the surface layer, carbon atoms preferred to precipitate from Ni, rather than from Cu, when the Cu atoms occupied some positions to reduce the proportion of Ni atoms, the precipitation of carbon atoms was also reduced and the few-layer graphene can be formed. For the situation of high Cu content, the laser processing should take the responsibility for invalid controllable growth. With the radiation of a high power density laser, the catalyst surface together with the as-coated carbon is heated at a rate of up to  $10^4$  °C/s to a temperature of around 2000 °C, forming a bath to dissolve carbon source and then cools down to precipitate carbon atoms and form graphene films. All the process was implemented in the open environment. At high temperature, Cu atoms are likely to combine the oxygen to form CuO. The high content of O in Cu35 is shown in Fig. 6e. It is not difficult to infer that there is more oxygen in Cu50 and Cu75. Therefore, the positions of original Cu has changed into the CuO, which cannot contribute to the growth of graphene. So there is no more graphene in the area where Cu atoms should be but

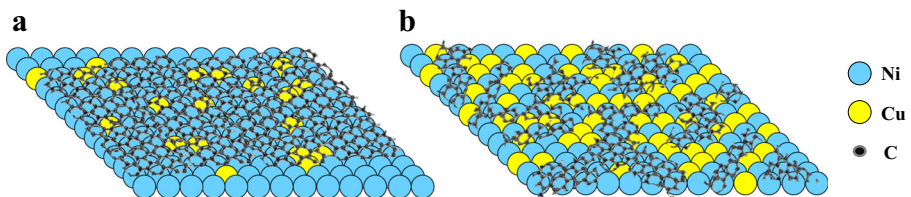


**Fig. 7** Mechanism of graphene layer control. **a** The growth of graphene in the catalyst with lower Cu content. **b** The growth of graphene in the catalyst with higher Cu content

actually CuO occupied. It results in the discontinuous graphene growth. When Cu atoms occupy most of the surface, the graphene growth can be completely restrained, as seen in Figs. 5f, g, m and n.

## Conclusions

We have succeeded in developing an engineering approach for the controllable graphene growth by laser process at room temperature. A high power fiber laser was used for Ni-Cu alloy preparation and controllable graphene growth. Different Ni-Cu alloy catalysts were formed in a high rate of  $720 \text{ mm}^2/\text{min}$  with a thickness of 1.2 mm. EDS analysis showed that the catalysts remained a uniform surface without defects. Then the graphene with controllable layers was rapidly and locally grown on the Ni-Cu catalysts by laser irradiation at a high rate ( $18 \text{ cm}^2/\text{min}$ ). The topographies of the samples displayed that Cu5 and Cu15 are the better catalysts than others, owing to the continuous formation and less wrinkles. Raman and AES results showed Cu15 was the most appropriate catalyst to grow the single layer graphene, which occupied 92.4 % of entire film. The catalysts with higher Cu content would not be workable to control the graphene layers, mainly due to the oxygen involved during the growth process.

**Acknowledgments** The authors greatly thank the funding support by China National Key Basic Research and Development Program (2011CB013000).

## References

1. Novoselov, K.S., Geim, A.K., Morozov, S.V., Jiang, D., Zhang, Y., Dubonos, S.V., et al.: Electric field effect in atomically thin carbon films. *Science* **306**, 666–669 (2004)
2. Novoselov, K.S., Fal'Ko, V.I., Colombo, L., Gellert, P.R., Schwab, M.G., Kim, K.: A roadmap for graphene. *Nature* **490**, 192–200 (2012)
3. Ferrari, A.C., Basko, D.M.: Raman spectroscopy as a versatile tool for studying the properties of graphene. *Nat. Nanotechnol.* **8**, 235–246 (2013)
4. Zang, J.F., Ryu, S., Pugno, N., Wang, Q.M., Tu, Q., Buehler, M.J., et al.: Multifunctionality and control of the crumpling and unfolding of large-area graphene. *Nat. Mater.* **12**, 321–325 (2013)
5. Neto, A.C., Guinea, F., Peres, N.M.R., Novoselov, K.S., Geim, A.K.: The electronic properties of graphene. *Rev. Mod. Phys.* **81**, 109 (2009)
6. Liu, H., Huang, J., Li, X., Liu, J., Zhang, Y., Du, K.: Flower-like  $\text{SnO}_2$ /graphene composite for high-capacity lithium storage. *Appl. Surf. Sci.* **258**, 4917–4921 (2012)
7. Kim, K.S., Zhao, Y., Jang, H., Lee, S.Y., Kim, J.M., Kim, K.S., et al.: Large-scale pattern growth of graphene films for stretchable transparent electrodes. *Nature* **457**, 706–710 (2009)
8. Dean, C.R., Young, A.F., Meric, I., Lee, C., Wang, L., Sorgenfrei, S., et al.: Boron nitride substrates for high-quality graphene electronics. *Nat. Nanotechnol.* **5**, 722–726 (2010)
9. Chen, S.S., Brown, L., Levendorf, M., Cai, W.W., Ju, S.Y., Edgeworth, J., et al.: Oxidation resistance of graphene-coated Cu and CuNi alloy. *ACS Nano* **5**, 1321–1327 (2011)
10. Ferrari, A.C., Meyer, J.C., Scardaci, V., Casiraghi, C., Lazzeri, M., Mauri, F., et al.: Raman spectrum of graphene and graphene layers. *Phys. Rev. Lett.* **97**, 187401 (2006)
11. Ni, Z., Wang, Y., Yu, T., Shen, Z.: Raman spectroscopy and imaging of graphene. *Nano Res.* **1**, 273–291 (2008)
12. Casiraghi, C., Hartschuh, A., Lidirikis, E., Qian, H., Harutyunyan, H., Gokus, T., et al.: Rayleigh imaging of graphene and graphene layers. *Nano Lett.* **7**, 2711–2717 (2007)
13. Nair, R.R., Blake, P., Grigorenko, A.N., Novoselov, K.S., Booth, T.J., Stauber, T., et al.: Fine structure constant defines visual transparency of graphene. *Science* **320**, 1308 (2008)

14. Chen, S., Cai, W., Piner, R.D., Suk, J.W., Wu, Y., Ren, Y., et al.: Synthesis and characterization of large-area graphene and graphite films on commercial Cu–Ni alloy foils. *Nano Lett.* **11**, 3519–3525 (2011)
15. Liu, X., Fu, L., Liu, N., Gao, T., Zhang, Y., Liao, L., Liu, Z.: Segregation growth of graphene on Cu–Ni alloy for precise layer control. *J. Phys. Chem. C* **115**, 11976–11982 (2011)
16. Zhang, Y., Tang, T.T., Girit, C., Hao, Z., Martin, M.C., Zettl, A., et al.: Direct observation of a widely tunable bandgap in bilayer graphene. *Nature* **459**, 820–823 (2009)
17. Partoens, B., Peeters, F.M.: From graphene to graphite: electronic structure around the K point. *Phys. Rev. B* **74**, 075404 (2006)
18. Ohta, T., Bostwick, A., Seyller, T., Horn, K., Rotenberg, E.: Controlling the electronic structure of bilayer graphene. *Science* **313**, 951–954 (2006)
19. Craciun, M.F., Russo, S., Yamamoto, M., Oostinga, J.B., Morpurgo, A.F., Tarucha, S.: Trilayer graphene is a semimetal with a gate-tunable band overlap. *Nat. Nanotechnol.* **4**, 383–388 (2009)
20. Liu, N., Fu, L., Dai, B., Yan, K., Liu, X., Zhao, R., et al.: Universal segregation growth approach to wafer-size graphene from non-noble metals. *Nano Lett.* **11**, 297–303 (2010)
21. Dai, B., Fu, L., Zou, Z., Wang, M., Xu, H., Wang, S., Liu, Z.: Rational design of a binary metal alloy for chemical vapour deposition growth of uniform single-layer graphene. *Nat. Commun.* **2**, 522 (2011)
22. Weatherup, R.S., Bayer, B.C.: In situ characterization of alloy catalysts for low-temperature graphene growth. *Nano Lett.* **11**, 4154–4160 (2011)
23. Ye, X., Long, J., Lin, Z., Zhang, H., Zhu, H., Zhong, M.: Direct laser fabrication of large-area and patterned graphene at room temperature. *Carbon* **68**, 784–790 (2014)
24. Li, X., Cai, W., Colombo, L., Ruoff, R.S.: Evolution of graphene growth on Ni and Cu by carbon isotope labeling. *Nano Lett.* **9**, 4268–4272 (2009)
25. Vilar, R.: Laser cladding. *J. Laser Appl.* **11**, 64–79 (1999)
26. Gao, W., Zhao, S., Liu, F., Wang, Y., Zhou, C., Lin, X.: Effect of defocus manner on laser cladding of Fe-based alloy powder. *Surf. Coat. Tech.* **248**, 54–62 (2014)
27. Zang, Z., Nakamura, A., Temmyo, J.: Single cuprous oxide films synthesized by radical oxidation at low temperature for PV application. *Opt. Express* **21**, 11448–11456 (2013)
28. Chen, H., Zhu, W., Zhang, Z.: Contrasting behavior of carbon nucleation in the initial stages of graphene epitaxial growth on stepped metal surfaces. *Phys. Rev. Lett.* **104**, 186101 (2010)
29. Wood, J.D., Schmucker, S.W., Lyons, A.S., Pop, E., Lyding, J.W.: Effects of polycrystalline Cu substrate on graphene growth by chemical vapor deposition. *Nano Lett.* **11**, 4547–4554 (2011)
30. Zhang, Y., Gomez, L., Ishikawa, F.N., Madaria, A., Ryu, K., Wang, C., et al.: Comparison of graphene growth on single-crystalline and polycrystalline Ni by chemical vapor deposition. *J. Phys. Chem. Lett.* **1**, 3101–3107 (2010)
31. Li, Y., Li, M., Gu, T., Bai, F., Yu, Y., Trevor, M., Yu, Y.: An important atomic process in the CVD growth of graphene Sinking and up-floating of carbon atom on copper surface. *Appl. Surf. Sci.* **284**, 207–213 (2013)